

RADNet: A Deep Neural Network Model for Robust Perception in Moving Autonomous Systems

Burhan A. Mudassar, Sho Ko, Maojingjing Li, Priyabrata Saha, Saibal Mukhopadhyay

Abstract—Interactive autonomous applications require robustness of the perception engine to artifacts in unconstrained videos. In this paper, we examine the effect of camera motion on the task of action detection. We develop a novel ranking method to rank videos based on the degree of global camera motion. For the high ranking camera videos we show that the accuracy of action detection is decreased. We propose an action detection pipeline that is robust to the camera motion effect and verify it empirically. Specifically, we do actor feature alignment across frames and couple global scene features with local actor-specific features. We do feature alignment using a novel formulation of the Spatio-temporal Sampling Network (STSN) but with multi-scale offset prediction and refinement using a pyramid structure. We also propose a novel input dependent weighted averaging strategy for fusing local and global features. We show the applicability of our network on our dataset of moving camera videos with high camera motion (MOVE dataset) with a 4.1% increase in frame mAP and 17% increase in video mAP.

I. INTRODUCTION

Interactive robotic and autonomous applications require detecting objects as well as the actions being performed by them [15], [21]. For example, an autonomous car not only needs to detect pedestrians but the action being performed by them to determine its own course of action. Action detection is an important component of the perception engine and it has received considerable progress in recent years due in part to deep-learning based architectures. The effective solutions repurpose deep learning based object detection architectures such as Faster RCNN and SSD and add temporal information to them [12], [16], [20], [22], [24], [26], [27], [37]. Yet, despite such advances, spatio-temporal action detection in unconstrained environments remains a hard problem due to video-specific artifacts such as motion blurring and jitter. Particularly for moving platforms, a common cause for the above artifacts is due to relative motion between the actor and the camera. Previously, camera motion has only been explored in the context of the task of action classification [2], [14], [31], [34] and not action detection. In this work, we take a step towards understanding the role of camera motion in action detection and computational steps to achieve robustness to it.

We focus on the task of spatio-temporal action detection in videos with high amounts of camera motion. To quantify the degree of camera motion we propose a novel ranking method that uses dense optical flow. Next, we observe that

current action detection models fail in challenging videos with high amounts of camera motion. We hypothesize the reduction in accuracy is due to reduced amounts of overlap of features of the actor across frames and the absence of discriminative actor features. Inspired by camera motion compensated features for action classification [2], [14], [31], we propose the addition of a fully learnable feature alignment module that predicts spatiotemporal offsets and uses deformable convolutions for compensation [3]. The concept of deformable convolutions for feature alignment is motivated by the STSN which predicts offsets at a single scale but unlike the STSN we predict offsets at multiple scales and propose a novel offset refinement step by creating a pyramid of offsets. In addition to that, we propose the addition of contextual information [18], [39] but with a novel input-dependent weighted averaging strategy for fusion of local and global features. We propose RADNet, a clip-based action detection architecture that takes in a stacked set of frames $f_t \dots f_{t+k}$ and generates feature maps at various scales (specifically 6 here) for all the frames within the clip. The feature maps at each scale and at each time step are aligned with respect to a reference frame within the clip using our multi-scale deformable convolution and refinement procedure. The aligned features are then fused with global scene features which are then used for prediction.

Once trained, our model can handle arbitrary camera motions, an idea that we verify by training on existing action detection datasets (UCF101-24 [29]) and evaluating on videos with high camera motion. We create a custom dataset of real-world moving camera videos with spatio-temporal annotation of actions. These videos comprise our *MOVE dataset*, which we will release. These videos contain a diverse array of actions in challenging scenarios with high degrees of camera motion. We verify the camera motion both qualitatively and quantitatively using our ranking method. Empirically, we observe that our model improves frame mAP and video mAP by 4.1% and 17% respectively on the MOVE dataset. The experiment validates that once trained on any action detection dataset, our model can be generalized to consider arbitrary camera motion.

In summary, our contributions are

- We construct a novel ranking method for quantifying degree of camera motion within a video and characterize the effect of camera motion on the accuracy of action detection.
- We propose a feature alignment module that predicts offsets at multiple scales and refines them by creating

All authors are affiliated with the School of ECE, Georgia Institute of Technology, Atlanta, GA, USA. Email: {burhan.mudassar, mli399, sko45, priyabratasaha}@gatech.edu, saibal@ece.gatech.edu

a pyramid of offsets.

- We propose a novel global feature fusion strategy that uses weighted averaging of local and global features.
- We propose a combined model with feature alignment and global feature fusion that improves overall action detection accuracy.
- We collect a dataset of challenging internet videos (MOVE dataset) with high degree of camera motions and annotate the actions within them and show the efficacy of our proposed network on it.

II. RELATED WORK

Action Detection The effective approach in literature is to adapt object detection architectures such as RCNN and SSD and incorporate temporal information to the architecture [8], [10], [12], [16], [20], [22], [23], [25], [26], [33], [37]. The temporal information is added either by adding optical flow as an additional modality to create a two-stream framework [10] or by processing a stack of frames [16], [22], [26] or by using 3D CNNs as feature extractors [11], [13], [36].

In fully supervised approaches, ROAD [27] is a single frame approach using SSD networks trained with annotated actions. ACT [16] and TRAMNet [26] are SSD-based architectures while AMTNet [22] and TPN [12] are Faster R-CNN-based architectures that use multiple frames. In addition, multi-task formulations [25], [28], recurrent classifiers [18] and early/hybrid fusion of optical flow and RGB [35], [37] are used to improve the action detection performance. The tubelet or frame level detections from these models are linked together to form action tubes through various methods including EM/Viterbi [16], [23], [27] tracking by detection [33] or learning-based [35]. This paper uses the ACT model [16] for benchmarking on action detection in moving camera sequences as it is a simple and powerful baseline.

Actions in Moving Camera Sequences The role of camera motion has been studied for action classification [2], [31], [34]. These approaches separate out camera-induced and object-induced features such as superpixels [2], dense trajectories [31] through homography [2], [31] or low-rank optimization [34]. Other approaches include using human detectors [21] or a CRF [30] to crop object boundaries and use the cropped features to perform classification. **However, Action detection in moving camera sequences has not received much attention in prior work.**

Datasets Action detection datasets contain both spatial and temporal labelling of actions. JHMDB-21 [6] contains

928 clips of 21 everyday actions such as *catch*, *pick*, *walk*, and *wave*. UCFSports [29] contains 150 videos of 10 sports-based actions such as *diving*, *running*, *kicking*. UCF101-24 [29] is a challenging dataset of 3207 untrimmed videos with 24 actions. The actions in UCF101-24 are also sports-centric i.e. *diving*, *cricket*, *diving*, *biking*, etc. AVA [11] is a large-scale dataset of over 80 actions in 430 15-minute video clips. **The videos in these datasets are either captured from a static viewpoint or have very smooth camera motions.**

A. Our contributions in Context of Prior Work

A summary of the qualitative comparisons with prior work is given in Table I.

Feature Alignment in Video Data: FGFA [38] aligns features from multiple frames to a keyframe by using optical flow based warping. In STSN [3] the optical flow warping step is replaced with deformable convolutions [7]. DT&T [9] track the detected objects and use cross-correlated feature maps for detection. Non-local Neural Networks [32] do non-local mean filtering over space and time for video action classification. Lei et al. use deformable temporal operations in which they predict temporal offsets for selecting feature maps for prediction [17] but they do not predict spatial offsets.

Our automated feature alignment step is most similar to the STSN [3] proposed for video object detection. The key difference is that we generate offsets at multiple scales. Additionally, we refine the offsets by upsampling the coarse offsets and adding to the finer-scale offsets similar to a pyramid. The pyramid approach is similar to FPN [19] but we create a pyramid of offsets and not features. An orthogonal approach is used by TramNET [26] that aligns the final predicted boxes. Unlike their approach we do the alignment step at the feature map level.

Global Features: Average fusion of scene and local features is used in CoupleNet [39] and RTPR [18] does concatenation of the local and global feature maps. We develop a weighted averaging scheme for fusion.

III. ACTION DETECTION IN MOVING CAMERA SEQUENCES

We focus on the problem of action detection for moving camera sequences. First, we develop a camera motion detection model based on dense optical flow. The videos containing actions are then ranked with the camera motion

Method	Global Features	Feature Alignment	End Task
CoupleNet [39]	Concat	-	Frame Object Detection
FGFA [38]	-	Optical Flow Warping	Video Object Detection
STSN [3]	-	Deformable Convolutions Single Scale	Video Object Detection
TramNET [26]	-	Proposal linking	Video Action Detection
RTPR [18]	Concat	-	Video Action Detection
This Work	Weighted Avg.	Deformable Convolutions. Refinement using Pyramids	Video Action Detection

TABLE I
COMPARISON WITH PRIOR WORK



Fig. 1. Some sample frames from the videos in the MOVE dataset. The videos contain diverse actions but with strong camera motion and jitter that leads to video artifacts such as motion blurring.



Fig. 2. A video after image stabilization. The movement of the borders shows the level of compensation applied to stabilize the video

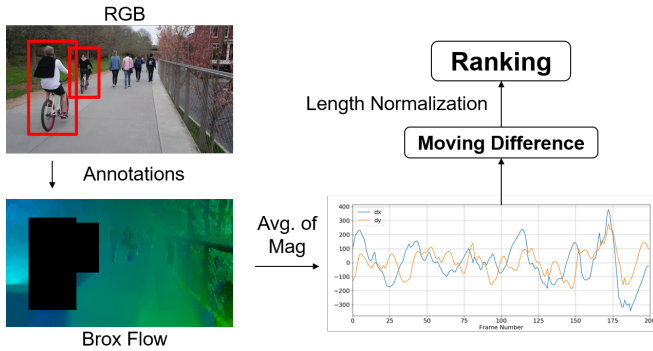


Fig. 3. Model for ranking videos by camera motion content

model. A baseline action detector is used to benchmark the action detection metrics.

A. Camera Motion Detection Model

Our model relies on dense optical flow to model the global camera motion between frames (Figure 3). The dense optical flow is computed using the Brox Method [5]. The average magnitude of the optical flow is stored for each frame (since we do not care about the direction of the apparent motion). Next, regions containing human motions are masked out as they are not always in agreement with the camera motion and may even provide erroneous estimates [31]. The masking is performed using the bounding box annotations. A moving difference of the average flow is taken and normalized by the length of the video to generate the ranking (Equations 1 and 2). Videos with a higher ranking are considered to have a higher degree of camera motion. We verify the ranking through visual inspection.

$$flow(t) = \frac{1}{x * y} * \sum_x \sum_y ||I_{masked}(t, x, y)|| \quad (1)$$

$$rank = \frac{1}{nframes} * \sum_{i=1}^{nframes-1} |flow(i+1) - flow(i)| \quad (2)$$

We compared our ranking with a video stabilization algorithm that uses Shi-Tomasi Corner Features and Pyramid Lucas-Kanade flow [1]. The stabilization transforms are

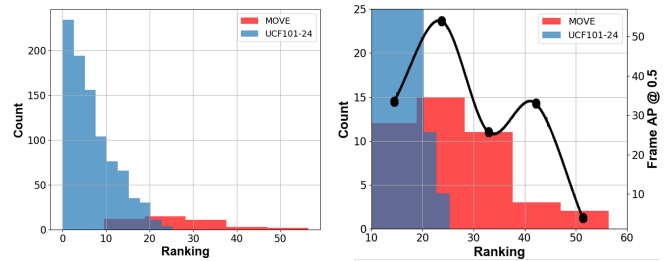


Fig. 4. Left: Histogram of videos ranked according to the degree of camera motion content. Right: Zoomed area shows count of videos with larger camera motion content and the black line shows frame AP at a threshold of 0.5 for the different clusters on the MOVE dataset with the baseline ACT ResNet50.

summed up and length normalized to generate the video ranking. Our ranking method gave a higher ranking to videos with jitter and irregular camera motions. The top ranking videos in the UCF-101-24 dataset with both rankings are shown in the supplementary material.

B. MOVE: A Dataset of Moving Camera Sequences

The camera motion ranking model shows that only a small subset of videos in the UCF101-24 dataset contains videos with high degree of camera motion. This motivates us to collect videos containing actions and with natural camera motions. We collected a dataset of moving camera videos from Youtube to empirically evaluate performance of action detection models on real-world sequences with natural camera motion. We chose videos containing activities that overlapped with the UCF-101-24 dataset and we collected 43 sequences with various actions and high degrees of camera motion. Some of these sequences are shown in Figure 1. A sample video is also shown with video stabilization applied to it in Figure 2 to show the degree of camera motion present. In these videos, actions were annotated spatially and temporally. Of the 24 actions present in UCF-24, we were able to collect videos containing 15 of those actions with clip lengths varying from 2 to 12 seconds. A comparison of the rankings for videos in UCF101-24 and the MOVE dataset in Figure 4 shows the stark difference in estimated motion for

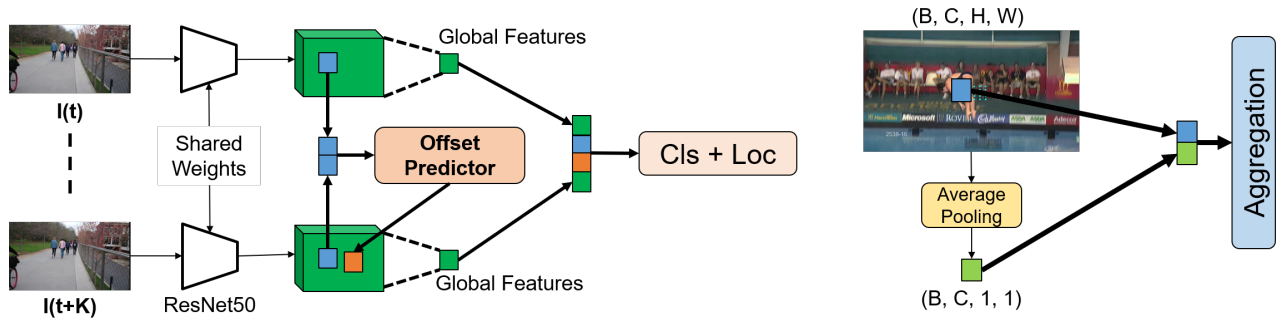


Fig. 5. The RADNet action detection model tailored for detection in moving camera sequences. Feature alignment is done by predicting likely locations of the objects in different frames using an offset predictor and the global scene features are aggregated with the local actor features.

the videos in UCF101-24 and our dataset. Over 23 videos in our dataset rank higher than the highest ranked videos in UCF101-24. **Our objective is not to train on this data but to simply use for evaluation.**

IV. THE RADNET MODEL

The RADNet model for action detection builds upon the ACT [16] framework for action detection. The network uses a stacked set of frames (clip/tubelet) to generate predictions. For each frame within the clip, feature maps (at multiple scales for one-stage detection) are generated by applying a convolutional backbone to the input frames and the generated feature maps (at the same scale) are combined together in the time dimension. Anchor cuboids are generated a priori for each location in the feature map by extending anchor boxes in the same spatial location over time. For each anchor cuboid, box regression and action classification is performed. The key difference is the addition of two layers. An automated feature alignment layer with multi-scale refinement spatially aligns features from multiple frames while a global feature fusion layer incorporates contextual information with local-actor specific features.

A. Feature Alignment with Multi-Scale Refinement

The feature alignment step aligns features spatially across the time dimension. Formally, given a stacked set of features $X_{stacked}$ corresponding to a stacked set of frames through timesteps $N - K$ to N , a prediction module M makes class predictions and localizations for every point (i, j) on that feature map (Equation 4) for time step N .

$$X_{stacked} = DepthConcat(X_{N-K}, X_{N-K+1}, \dots, X_N) \quad (3)$$

$$cls, loc(N, i, j) = M(X_{stacked}) \quad (4)$$

For a point on the feature map (i, j) our objective is to transform X_{N-K} through X_N so that features relevant to (i, j) are passed through (Equation 5). The transformation is achieved by tuning the receptive field of the filters at that location by adding an offset from the set of predicted offsets ΔP .

$$X(t, i, j) = \sum X(t, p + \Delta p(t, i, j)), t \in T \quad (5)$$

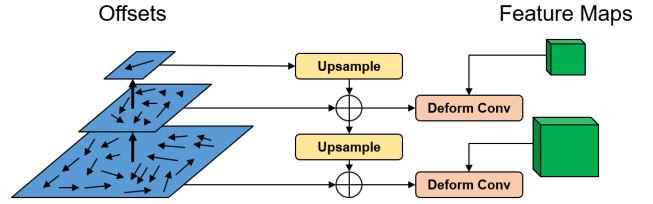


Fig. 6. Refinement of predicted offsets at different scales

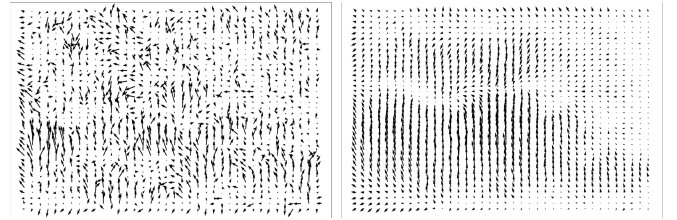


Fig. 7. Before and after refinement of offsets at the finest scale

The set of offsets ΔP is computed from the stacked set of feature maps $X_{stacked}$ for every point in the sampling grid G . Let F be the function that predicts offsets for each time step for every spatial point in the feature map. We apply F to get ΔP as shown in Equation 6.

$$\Delta P = F(X_{stacked}) \quad (6)$$

F can be any transformation such as optical flow between frames. For a fully end-to-end learning framework, F needs to be differentiable. The STSN framework using deformable convolutions is adopted to model F . Briefly, a 2D convolution layer predicts offsets which are then used to offset the sampling locations for the convolution operator. However, convolution is a very local operation with limited receptive fields i.e. 3×3 and cannot model the global camera motion effectively. The solution is to create a pyramid representation of the offsets. The formulation for the pyramid is trivial [4] and is adapted to RADNet as follows.

Let O be the set of offsets with o^k being the offsets computed at the k th scale. In SSD, the feature maps at 6 scales are used for prediction thus there are 6 levels of offsets in O with scales ranging from 38×38 to 1×1 . The offsets at the coarsest scale (1×1) model the average

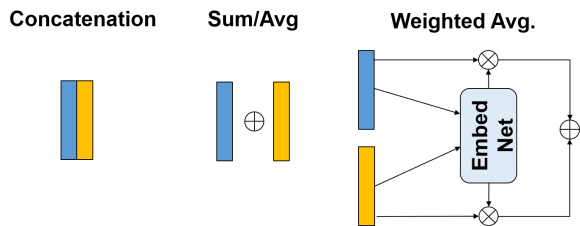


Fig. 8. Aggregation strategies for local features and global features

camera motion component. They are then upsampled and added to the finer scales recursively. The up-sampled is performed using bilinear sampling. The block diagram for the refinement is shown in Figure 6. A qualitative comparison before and after refinement is shown in Figure 7. The noisy local motion components are smoothed using the refinement procedure.

B. Global and Local Feature Fusion

To incorporate contextual information, we extract features corresponding to the whole scene and fuse them with the local actor specific features f_{local} . The global features f_{global} are generated by average pooling the feature map at that scale. The global feature map is then aggregated with the local feature maps for prediction. Multiple fusion strategies for aggregation are implemented including concatenation, averaging and weighted averaging as shown in Figure 8.

1. Concatenation In this scheme, the local and global feature maps are concatenated along the channel dimension. The width of the next layer needs to be doubled to accommodate this.

2. Average/Summation The local and global feature maps are averaged or summed up along the channel dimension. The width of the next layer does not change in this scheme.

3. Weighted Averaging A novel weighted averaging scheme is implemented that dynamically weighs the global and local features for every input sample and for every input spatial location. The weighted averaging is implemented by using an embedding function to generate weights for the actor features and global features. Formally let the embedding function be f_{embed} and let the actor features weight be l^i and the global feature be g^i for the i th input sample. The embeddings for both are generated by applying f_{embed} as given in Equation 7.

$$l_{embed}^i, g_{embed}^i = f_{embed}(l^i), f_{embed}(g^i) \quad (7)$$

The normalized weight embeddings $w_{normalized}^i$ are then generated by applying the softmax function over concatenation of l_{embed} and g_{embed} (Equation 8).

$$w_{normalized}^i = softmax(concat(l_{embed}^i, g_{embed}^i)) \quad (8)$$

The $w_{normalized}$ is then used to do the weighted summation of the global and local features as given in Equation 9 to get the output feature map p for prediction.

$$p^i = l^i * w_{normalized}^i[0] + g^i * w_{normalized}^i[1] \quad (9)$$

detector	method	JHMDB-21		UCF-101-24	
		0.2	0.5:0.95	0.2	0.5:0.95
SSD	ROAD [27]	73.8	41.6	73.5	20.4
	ACT [16]	74.2	44.8	76.5	23.4
	TramNet $\Delta 1$ [26]	-	-	79.0	23.9
	AMTNet-L [26]	-	-	79.4	23.4
	TACNET [28]	74.1	44.8	77.5	24.1
	ours	75.1	48.3	78.4	24.5

TABLE II

COMPARISON RESULTS ON VIDEO MAP OF OUR METHOD TO THE STATE OF THE ART AT VARIOUS DETECTION THRESHOLDS.

We use a 3 layer DNN [38] EmbedNet to implement the f_{embed} function. The EmbedNet takes in the local features and the global features of dimension (B, C, H, W) . The output of EmbedNet is a one-channel feature map $(B, 1, H, W)$. The local and global embeddings are then concatenated and the softmax is applied to get a normalized weighted feature map. The global and local weights are then multiplied with the global and local features respectively.

V. EXPERIMENTAL RESULTS AND ANALYSIS

We evaluate the different configurations of RADNet on the MOVE Dataset. In addition, we also benchmark RADNet on existing action detection datasets JHMDB-21 and UCF101-24. For accuracy benchmarking, frame AP and video AP metrics are used. Frame AP evaluates correctness of detections only at the frame level while video AP checks for temporal consistency of detections for the duration of the video.

Implementation Details : We use the ResNet-50 backbone in all of our models. 3 extra residual blocks are added and feature maps from res3, res4, res5 and the extra layers are used. All images are resized to 300 x 300 for training and testing. The model is trained with a step learning schedule and a starting learning rate of 1e-3 for a total of 130000 iterations and a batch size of 8. The feature alignment layers are added to the output of all scales.

Network	frameAP		Video mAP	
	0.5	0.1	0.2	0.3
ACT ResNet-50	27.7	57.8	52.3	48.7
Feature Alignment				
+STSN [3]	27.1	55.9	50.5	43.9
+STSN+refinement	31.1	67.2	63.9	57.7

TABLE III

COMPARISON ON THE MOVE DATASET WITH AND WITHOUT FEATURE ALIGNMENT

A. Evaluation on Existing Datasets

Evaluation of video mAP on the UCF101-24 and JHMDB-21 datasets (Table II) is performed. For direct comparison, both RGB and optical flow modalities are used and we use the two-stream network formulation [10]. Similar to prior work, we average the results for all splits for JHMDB and for UCF101 we report the results for the first split only. For the JHMDB dataset, we improve the video mAP at all thresholds.

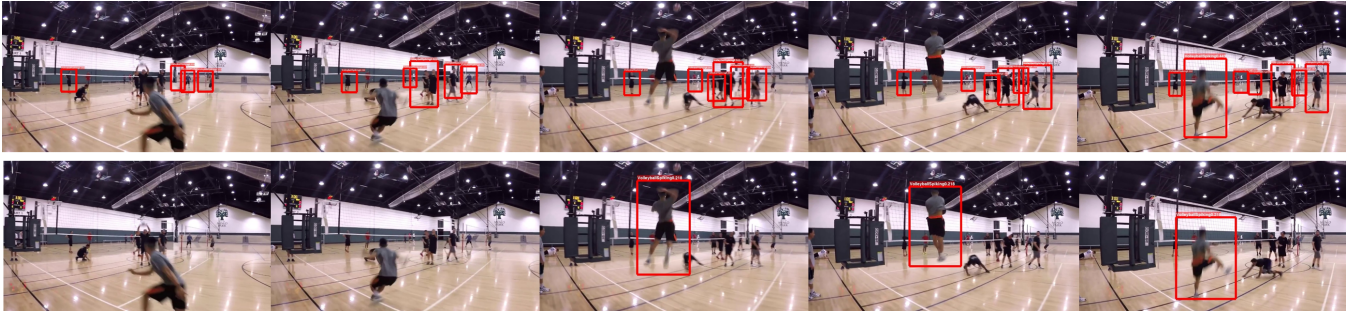


Fig. 9. Results on the MOVE dataset after post-processing of detections. Only the action labelled for the video is shown for visual clarity. Top Row: With the ACT detector. Bottom: Our model. In the volleyball video, the ACT detector does not detect the correct actor and has many false positives

Network	frameAP	Video mAP		
	0.5	0.1	0.2	0.3
ACT ResNet-50	27.7	57.8	52.3	48.7
Global Feature Fusion				
Concat	29.0	54.6	48.6	46.7
Avg	29.4	59.9	56.4	45.0
Weighted Avg	29.2	66.1	60.5	51.9

TABLE IV

COMPARISON ON THE MOVE DATASET WITH AND WITHOUT GLOBAL FEATURE FUSION

STSN [3]	global	refinement	frame AP	Params	FLOPS
			27.7	35.5	17.5
✓			27.1	93.1	39.1
✓		✓	31.1	93.1	39.1
	✓		29.2	63.6	28.9
✓	✓		31.6	121.4	49.6
✓	✓	✓	31.8	121.4	49.6

TABLE V

ABLATION STUDY ON THE MOVE DATASET

For UCF101-24, we improve the video mAP at at 0.5:0.95 by 0.4%. The small increase in video mAP is attributed to the fact that the datasets contain few moving camera videos so our network does not improve the performance by much.

B. Evaluation on MOVE Dataset

Evaluation on the MOVE dataset is only performed on the RGB images and with the RGB-trained network.

Feature Aligement The effect of feature alignment is discussed here (Table III). In the first experiment the STSN module without refinement is added to the network. The accuracy metrics are decreased. We attribute this to the

Network	frameAP	Video mAP		
	0.5	0.1	0.2	0.3
ACT ResNet-50	27.7	57.8	52.3	48.7
RADNet	31.8	74.9	70.8	65.7

TABLE VI

COMPARISON ON THE MOVE DATASET WITH RADNET AND PRIOR WORK

inaccurate offsets being computed. With the addition of the refinement the frame AP is boosted by 3.4% and the video AP is also improved by 9.0% at a threshold of 0.3 This validates quantitatively the advantage of the refinement step. It also comes at a minimal cost with no addition in the parameters of the model.

Global Fusion Strategies: Next, the different global fusion strategies are evaluated in the network (Table IV). The weighted averaging shows a clear advantage over the concatenation and simple averaging with increase in video mAP (66.1% vs. 57.8%) at a threshold of 0.1 and 51.9% vs 48.7% at a threshold of 0.3.

Ablation Studies: Ablation studies were performed on the MOVE dataset with different configurations of the model (Table V). It is interesting to note that the combined STSN and global feature fusion model improve the frame AP more than their individual contributions. Thus, their effects are complementary. The weighted averaging scheme is used for fusion in all the configurations. The highest frame AP and video AP are observed with the offset refinement and weighted averaging global feature fusion (31.8%). For RADNet we use this configuration to compare with ACT and improve frame AP by 4.1% and video AP by 17% at a threshold of 0.3 (Table VI).

VI. CONCLUSION

In this paper, we have presented the problem of spatio-temporal action detection in moving camera sequences. We have collected and presented a test dataset containing moving camera sequences with annotated actions. We have shown a novel action detection architecture that is robust to the effect of camera motion in action detection. For future work, we intend to collect more videos for testing and possibly for training as well. In addition we will investigate the two-stream model for fusing optical flow input in the moving camera context. We hope that this will encourage further research into this domain.

ACKNOWLEDGEMENTS

The research reported here was supported in part by the Defense Advanced Research Projects Agency (DARPA) under contract number HR0011-17-2-0045. The views and conclusions contained herein are those of the authors and

should not be interpreted as necessarily representing the official policies or endorsements, either expressed or implied, of DARPA.

REFERENCES

- [1] A python package to stabilize videos using opencv. https://github.com/AdamSpannbauer/python_video_stab. Accessed: 2019-11-15. **3**
- [2] K. Avgerinakis, K. Adam, A. Briassouli, and Y. Kompatsiaris. Moving camera human activity localization and recognition with motionplanes and multiple homographies. In *Image Processing (ICIP), 2015 IEEE International Conference on*, pages 2085–2089. IEEE, 2015. **1, 2**
- [3] G. Bertasius, L. Torresani, and J. Shi. Object detection in video with spatiotemporal sampling networks. In *Proceedings of the European Conference on Computer Vision (ECCV)*, pages 331–346, 2018. **1, 2, 5, 6**
- [4] J.-Y. Bouguet et al. Pyramidal implementation of the affine lucas kanade feature tracker description of the algorithm. *Intel Corporation*, 5(1-10):4, 2001. **4**
- [5] T. Brox, A. Bruhn, N. Papenbergh, and J. Weickert. High accuracy optical flow estimation based on a theory for warping. In *European conference on computer vision*, pages 25–36. Springer, 2004. **3**
- [6] G. Chéron, I. Laptev, and C. Schmid. P-cnn: Pose-based cnn features for action recognition. In *Proceedings of the IEEE international conference on computer vision*, pages 3218–3226, 2015. **2**
- [7] J. Dai, H. Qi, Y. Xiong, Y. Li, G. Zhang, H. Hu, and Y. Wei. Deformable convolutional networks. In *Proceedings of the IEEE International Conference on Computer Vision*, pages 764–773, 2017. **2**
- [8] C. Feichtenhofer, A. Pinz, and A. Zisserman. Convolutional two-stream network fusion for video action recognition. In *Proceedings of the IEEE Conference on Computer Vision and Pattern Recognition*, pages 1933–1941, 2016. **2**
- [9] C. Feichtenhofer, A. Pinz, and A. Zisserman. Detect to track and track to detect. In *Proceedings of the IEEE International Conference on Computer Vision*, pages 3038–3046, 2017. **2**
- [10] G. Gkioxari and J. Malik. Finding action tubes. In *Proceedings of the IEEE conference on computer vision and pattern recognition*, pages 759–768, 2015. **2, 5**
- [11] C. Gu, C. Sun, D. A. Ross, C. Vondrick, C. Pantofaru, Y. Li, S. Vijayanarasimhan, G. Toderici, S. Ricco, R. Sukthankar, et al. Ava: A video dataset of spatio-temporally localized atomic visual actions. In *Proceedings of the IEEE Conference on Computer Vision and Pattern Recognition*, pages 6047–6056, 2018. **2**
- [12] J. He, Z. Deng, M. S. Ibrahim, and G. Mori. Generic tubelet proposals for action localization. In *2018 IEEE Winter Conference on Applications of Computer Vision (WACV)*, pages 343–351. IEEE, 2018. **1, 2**
- [13] R. Hou, C. Chen, and M. Shah. An end-to-end 3d convolutional neural network for action detection and segmentation in videos. *arXiv preprint arXiv:1712.01111*, 2017. **2**
- [14] M. Jain, H. Jegou, and P. Boutheymy. Better exploiting motion for better action recognition. In *Proceedings of the IEEE conference on computer vision and pattern recognition*, pages 2555–2562, 2013. **1**
- [15] Y. Jiang and A. Saxena. Modeling high-dimensional humans for activity anticipation using gaussian process latent crfs. In *Robotics: Science and systems*, pages 1–8, 2014. **1**
- [16] V. Kalogeiton, P. Weinzaepfel, V. Ferrari, and C. Schmid. Action tubelet detector for spatio-temporal action localization. *ICCV*, 2017. **1, 2, 4, 5**
- [17] P. Lei and S. Todorovic. Temporal deformable residual networks for action segmentation in videos. In *Proceedings of the IEEE Conference on Computer Vision and Pattern Recognition*, pages 6742–6751, 2018. **2**
- [18] D. Li, Z. Qiu, Q. Dai, T. Yao, and T. Mei. Recurrent tubelet proposal and recognition networks for action detection. In *Proceedings of the European conference on computer vision (ECCV)*, pages 303–318, 2018. **1, 2**
- [19] T.-Y. Lin, P. Dollár, R. Girshick, K. He, B. Hariharan, and S. Belongie. Feature pyramid networks for object detection. In *Proceedings of the IEEE conference on computer vision and pattern recognition*, pages 2117–2125, 2017. **2**
- [20] X. Peng and C. Schmid. Multi-region two-stream r-cnn for action detection. In *European Conference on Computer Vision*, pages 744–759. Springer, 2016. **1, 2**
- [21] F. Rezaadegan, S. Shirazi, B. Upcroft, and M. Milford. Action recognition: From static datasets to moving robots. In *Robotics and Automation (ICRA), 2017 IEEE International Conference on*, pages 3185–3191. IEEE, 2017. **1, 2**
- [22] S. Saha, G. Singh, and F. Cuzzolin. Amtnet: Action-micro-tube regression by end-to-end trainable deep architecture. In *Proceedings of the IEEE International Conference on Computer Vision*, pages 4414–4423, 2017. **1, 2**
- [23] S. Saha, G. Singh, M. Sapienza, P. H. Torr, and F. Cuzzolin. Deep learning for detecting multiple space-time action tubes in videos. In *Proceedings of the British Machine Vision Conference*, 2016. **2**
- [24] K. Simonyan and A. Zisserman. Two-stream convolutional networks for action recognition in videos. In *Advances in neural information processing systems*, pages 568–576, 2014. **1**
- [25] G. Singh, S. Saha, and F. Cuzzolin. Predicting action tubes. In *Proceedings of the European Conference on Computer Vision (ECCV)*, pages 0–0, 2018. **2**
- [26] G. Singh, S. Saha, and F. Cuzzolin. Tramnet-transition matrix network for efficient action tube proposals. In *Asian Conference on Computer Vision*, pages 420–437. Springer, 2018. **1, 2, 5**
- [27] G. Singh, S. Saha, M. Sapienza, P. H. Torr, and F. Cuzzolin. Online real-time multiple spatiotemporal action localisation and prediction. In *ICCV*, pages 3657–3666, 2017. **1, 2, 5**
- [28] L. Song, S. Zhang, G. Yu, and H. Sun. Tacnet: Transition-aware context network for spatio-temporal action detection. In *Proceedings of the IEEE Conference on Computer Vision and Pattern Recognition*, pages 11987–11995, 2019. **2, 5**
- [29] K. Soomro, A. R. Zamir, and M. Shah. Ucf101: A dataset of 101 human actions classes from videos in the wild. *arXiv preprint arXiv:1212.0402*, 2012. **1, 2**
- [30] P. Tokmakov, K. Alahari, and C. Schmid. Learning motion patterns in videos. In *Proceedings of the IEEE Conference on Computer Vision and Pattern Recognition*, pages 3386–3394, 2017. **2**
- [31] H. Wang and C. Schmid. Action recognition with improved trajectories. In *Proceedings of the IEEE international conference on computer vision*, pages 3551–3558, 2013. **1, 2, 3**
- [32] X. Wang, R. Girshick, A. Gupta, and K. He. Non-local neural networks. In *Proceedings of the IEEE Conference on Computer Vision and Pattern Recognition*, pages 7794–7803, 2018. **2**
- [33] P. Weinzaepfel, Z. Harchaoui, and C. Schmid. Learning to track for spatio-temporal action localization. In *Proceedings of the IEEE international conference on computer vision*, pages 3164–3172, 2015. **2**
- [34] S. Wu, O. Oreifej, and M. Shah. Action recognition in videos acquired by a moving camera using motion decomposition of lagrangian particle trajectories. In *2011 International conference on computer vision*, pages 1419–1426. IEEE, 2011. **1, 2**
- [35] X. Yang, X. Yang, M.-Y. Liu, F. Xiao, L. S. Davis, and J. Kautz. Step: Spatio-temporal progressive learning for video action detection. In *Proceedings of the IEEE Conference on Computer Vision and Pattern Recognition*, pages 264–272, 2019. **2**
- [36] Y. Zhang, P. Tokmakov, M. Hebert, and C. Schmid. A structured model for action detection. In *Proceedings of the IEEE Conference on Computer Vision and Pattern Recognition*, pages 9975–9984, 2019. **2**
- [37] J. Zhao and C. G. Snoek. Dance with flow: Two-in-one stream action detection. In *Proceedings of the IEEE Conference on Computer Vision and Pattern Recognition*, pages 9935–9944, 2019. **1, 2**
- [38] X. Zhu, Y. Wang, J. Dai, L. Yuan, and Y. Wei. Flow-guided feature aggregation for video object detection. In *Proceedings of the IEEE International Conference on Computer Vision*, volume 3, 2017. **2, 5**
- [39] Y. Zhu, C. Zhao, J. Wang, X. Zhao, Y. Wu, and H. Lu. Couplet: Coupling global structure with local parts for object detection. In *Proceedings of the IEEE International Conference on Computer Vision*, pages 4126–4134, 2017. **1, 2**